Analysis of $B \to \omega l \nu$ Decays With BaBar

Yiwen Chu[1], Bryce Littlejohn[2]

Office of Science, SULI Program

[1]Massachusetts Institute of Technology, [2]Principia College

Stanford Linear Accelerator Center

Menlo Park, California

August 29, 2005

Prepared in partial fulfillment of the requirements of the Office of Science, U.S. Department of Energy Science Undergraduate Laboratory Internship (SULI) Program under the direction of Jochen Dingfelder in Experimental Group C at the Stanford Linear Accelerator Center (SLAC).

Participants: _____

Signature

Research Advisor: _____

Signature

Work supported by Department of Energy contract DE-AC02-76SF00515

Contents

1 Abstract

Analysis of $B \to \omega l \nu$ Decays With BaBar. YIWEN CHU(Massachusetts Institute of Technology, Cambridge, MA 02139) BRYCE LITTLEJOHN(Principia College, Elsah, IL 62028) JOCHEN DINGFELDER(Stanford Linear Accelerator Center, Menlo Park, CA 94025).

As part of the BaBar project at SLAC to study the properties of B mesons, we have carried out a study of the exclusive charmless semileptonic decay mode $B \to \omega l \nu$, which can be used to determine the Cabbibo-Kobayashi-Maskawa matrix element V_{ub}. Using simulated event samples, this study focuses on determining criteria on variables for selection of $B \to \omega l \nu$ signal and suppression of background from other types of $B\bar{B}$ events and continuum processes. In addition, we determine optimal cuts on variables to ensure a good neutrino reconstruction. With these selection cuts, we were able to achieve a signal-to-background ratio of 0.68 and a signal efficiency of the order of 1%. Applying these cuts to a sample of 83 million $B\bar{B}$ events recorded by BaBar in e^+e^- collisions at the $\Upsilon(4S)$ resonance, we obtain a yield of 115 $\pm$ 19 $B \to \omega l \nu$ decays.

2 Introduction

The BaBar experiment at SLAC studies the properties of B mesons in $B\bar{B}$ events produced in e^+e^- collisions on the $\Upsilon(4S)$ resonance. We study the particular exclusive decay $B \to \omega l\nu$, which is called a charmless semileptonic decay due to the presence of two leptons and the ω meson in the final state. The study of charmless semileptonic decays allows for the determination of the Cabbibo-Kobayashi-Maskawa (CKM) matrix element $|V_{ub}|$, which determines the probability of a $b \to u$ transition in a weak interaction and is one of the smallest and least known elements. In the Standard Model, the

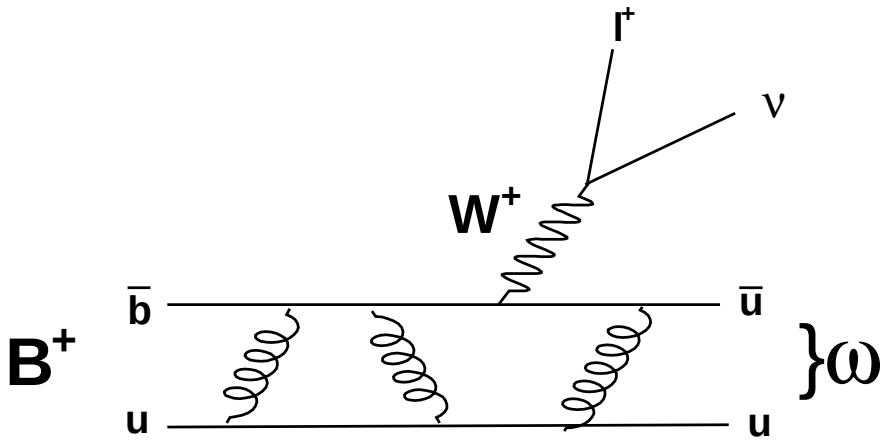

Figure 1: Feynman diagram of a $B \to \omega l\nu$ decay.

CKM matrix is unitary, and this condition can be graphically represented as the Unitarity Triangle in the complex $(\rho - \eta)$ plane [1]. $|V_{ub}|$ indicates the length of one side of this triangle. A precise measurement of $|V_{ub}|$ would significantly improve the constraints on the Unitarity Triangle and provide a stringent test of the Standard Model mechanism for Charge-Parity (CP) violation.

The BaBar collaboration has already measured several other charmless

semileptonic decays, such as $B \to \pi l\nu$ and $B \to \rho l\nu$ [2]. However, the $B \to \omega l\nu$ mode is experimentally more difficult and has not yet been studied in detail with sufficient signal statistics by BaBar. Recent studies at Belle have been able to identify these events and measure a branching fraction of $(1.3 \pm 0.4 \pm 0.3 \pm 0.3) \times 10^{-4}$ [3].

In this study, we focus on improving the selection of $B \to \omega l\nu$ decays by reducing the background from other processes and ensuring a reliable reconstruction of the neutrino kinematics. In the complex process of analyzing data, discrimination between signal and background is particularly important and challenging for a rare process such as $B \to \omega l\nu$. By looking at tracks made in different parts of the BaBar detector, we can reconstruct and identify the particles produced in the e^+e^- collision, thereby selecting signal decays. However, background events can be misidentified as signal, or a real signal decay may be wrongly reconstructed. The latter case may occur by, for example, assigning a particle from the other B decay to the signal B decay. Significant backgrounds include $B \to X_c l\nu$ decays, where X_c stands for a meson that contains a c quark, and $e^+e^- \to q\bar{q}$ processes ("continuum events"). Fortunately, the features of the signal events we are interested in differ in many ways from those of the background, which allows us to enhance the signal by applying selection cuts on variables that exhibit these differences. Another challenge of the analysis process involves the reliable reconstruction of the semileptonic decay kinematics. In particular, we study the quality of the neutrino reconstruction. Since these particles are not directly detectable, their kinematics must be inferred indirectly from the missing momentum and energy of the entire event, causing much room for error. We study several variables that can be used to ensure a good quality of the neutrino reconstruction.

After performing the above studies using Monte Carlo simulated samples, we can determine the number of signal events in a sample of 83 million $B\bar{B}$ events recorded with the BaBar detector.

3 Analysis Methods

To identify a $B \to \omega l\nu$ decay, we look for the presence of a lepton with center-of-mass momentum greater than 1.3 GeV/c, a substantial missing momentum as indication of a neutrino in the event, and a reconstructed hadron consistent with an ω meson. The ω is reconstructed in its dominant decay mode $\omega \to \pi^+\pi^-\pi^0$, where the π^+ and π^- are identified as charged tracks in the drift chamber not consistent with a lepton or kaon and the π^0 as two photons in the electromagnetic calorimeter produced in the decay $\pi^0 \to \gamma\gamma$.

The data and Monte Carlo samples used in our analysis have been applied with preliminary selection criteria ("preselection"). In order to reduce continuum background events that are not produced on the $\Upsilon(4S)$ resonance, the preselection uses loose cuts on the number of charged tracks ($N_{track} > 3$), $R2 < 0.6$, $|\cos\theta_{BY}| < 1.5$ (see section 3.2 for definitions of $R2$ and $|\cos\theta_{BY}|$). In addition, we apply a loose cut on the invariant mass of the three pions forming the omega candidate of $0.70 < m_{\pi^+\pi^-\pi^0} < 0.86$ GeV and a cut on the ω decay amplitude of the three pions produced, given by

$$\lambda = \frac{|\vec{p}_{\pi^+} \times \vec{p}_{\pi^-}|^2}{\frac{3}{4}(\frac{1}{9}m_{3\pi}^2 - m_{\pi^+}^2)^2} > 0.25 \text{ GeV}^{-2}. \quad (1)$$

These criteria significantly reduce the requirements on CPU time and disk space and yield a data sample of manageable size for this analysis.

3.1 Neutrino Reconstruction

In addition to the energetic charged lepton, the presence of a neutrino in the decay products of the B meson is a characteristic feature of semileptonic modes, so we first try to isolate events with a well reconstructed neutrino. Since neutrinos cannot be detected, we must infer their mass and kinematics from all reconstructed particles. The four-momentum of the neutrino is taken to be the missing four-momentum of the event, given by

$$(\vec{p}_\nu, E_\nu) = (\vec{p}_{miss}, E_{miss}) = (\vec{p}_{beams}, E_{beams}) - (\sum_i \vec{p}_i, \sum_i E_i), \tag{2}$$

where $\vec{p}_{beams}, E_{beams}$ are the sums of the known momenta and energies of the colliding e^+ and e^-, and $\vec{p}_i, E_i$ are the momentum and energy of the i^{th} reconstructed particle [4]. We also reject events with $|\vec{p}_{miss}| < 0.7$ GeV. The missing-mass squared of the neutrino is then calculated as

$$m^2_{miss} = E^2_{miss} - |\vec{p}^{\,2}_{miss}|. \tag{3}$$

In the simulated events, these reconstructed quantities can be compared to the true values for each event, which tells us how well the neutrino has been reconstructed. In particular, we are interested in the following resolutions:

1. $|\vec{p}_{miss}| - |\vec{p}_{\nu,true}|$: The difference in the magnitudes of the lab-frame momenta.

2. $q^2_{reco.} - q^2_{true}$: Here q^2 is the four-momentum transfer of the decay, given by

$$q^2 = (p_{lepton} + p_\nu)^2 = (p_B - p_{hadron})^2. \tag{4}$$

   It is equivalent to the invariant mass squared of the virtual W boson involved in the production of the lepton and neutrino.

We try to quantify the quality of the neutrino reconstruction by fitting the $|\vec{p}_{miss}| - |\vec{p}_{\nu,true}|$ distribution with a Gaussian function for the peak and

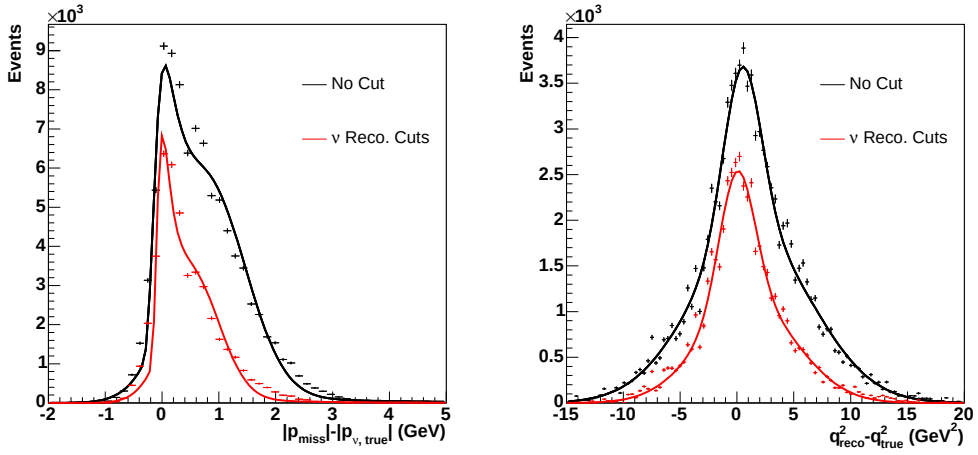

(a) (b)

Figure 2: Resolutions (a) $|\vec{p}_{miss}| - |\vec{p}_{\nu,true}|$ and (b) $q^2_{reco.} - q^2_{true}$. Crosses are simulated signal events with statistical error and lines are fits. Black: No cuts applied. Red: Resolutions after chosen cut of $\frac{m^2_{miss}}{E_{miss}} < 2.6$ GeV, $\theta_{miss} > 0.5$ rad, and $Q_{tot} \leq 1$.

a Landau function for the tail. The $q^2_{reco.} - q^2_{true}$ distribution was fitted with two Gaussian functions, one for the peak and the other to describe the tails. Although the fits are not perfect, they approximately quantify the quality of the reconstructed neutrino. We then study the width (σ_{peak}) and mean (μ_{peak}) of the peak Gaussian functions, along with the ratio $\frac{N_{tail}}{N_{all}}$, where N_{all} is the number of events in both the Gaussian and Landau functions, and N_{tail} is the number of events in the tail with selection criteria (as explained below) outside 2σ of the Gaussian peak without selection criteria.

As can be seen in Fig. 2, there are significant resolution tails due to poorly reconstructed events. These tails are mostly caused by events where particles are lost outside the detector acceptance region or by the production of an additional neutrino from, for example, the decay of the other B meson. By discarding events that do not satisfy selection criteria on the following

variables that are directly affected by the neutrino reconstruction, we can reduce the resolution tails.

1. $Q_{tot} = \sum_i Q_{track,i}$: If a charged particle was lost, the total charge of the event will generally no longer be zero. To reduce the effect of losses due to detector acceptance, we use the typical cut of $Q_{tot} \leq 1$.

2. m^2_{miss}/E_{miss}: m^2_{miss} should be $m^2_\nu = 0$. Since the m^2_{miss} resolution broadens linearly with E_{miss}, a cut on this variable is more effective than a cut on m^2_{miss}.

3. θ_{miss}: This variable indicates the angle between the missing momentum and the e^- beam. When this angle is close to 0^o or 180^o, it is likely that the missing momentum was caused by a particle other than a neutrino traveling in the direction of the beamline, where it cannot be detected.

We vary the cuts from $m^2_{miss}/E_{miss} < 1.0$ GeV to $m^2_{miss}/E_{miss} < 3.8$ GeV and from $\theta_{miss} > 0$ rad to $\theta_{miss} > 0.6$ rad and then plot the signal efficiency $\epsilon_{sig} = N^{sig}_{cut}/N^{sig}_{uncut}$ and the characteristic parameters of the resolutions as functions of cut values in order to find the best combination of cuts (see Fig 3). While we see only a moderate improvement when tightening the cut on the missing mass, a tighter cut on θ_{miss} significantly improves the resolution. We choose the cuts $m^2_{miss}/E_{miss} < 2.6$ GeV, $\theta_{miss} > 0.5$ rad, and $Q_{tot} \leq 1$. This optimum combination of cuts, along with other cuts of similar efficiency, are presented in Table 1 for comparison.

3.2 Background Suppression and Signal Selection

The background for $B \to \omega l\nu$ decays can be categorized into several sources. Continuum background consisting of $e^+e^- \to q\bar{q}$ processes are the largest contribution, while another significant source is semileptonic $B \to X_c l\nu$ events

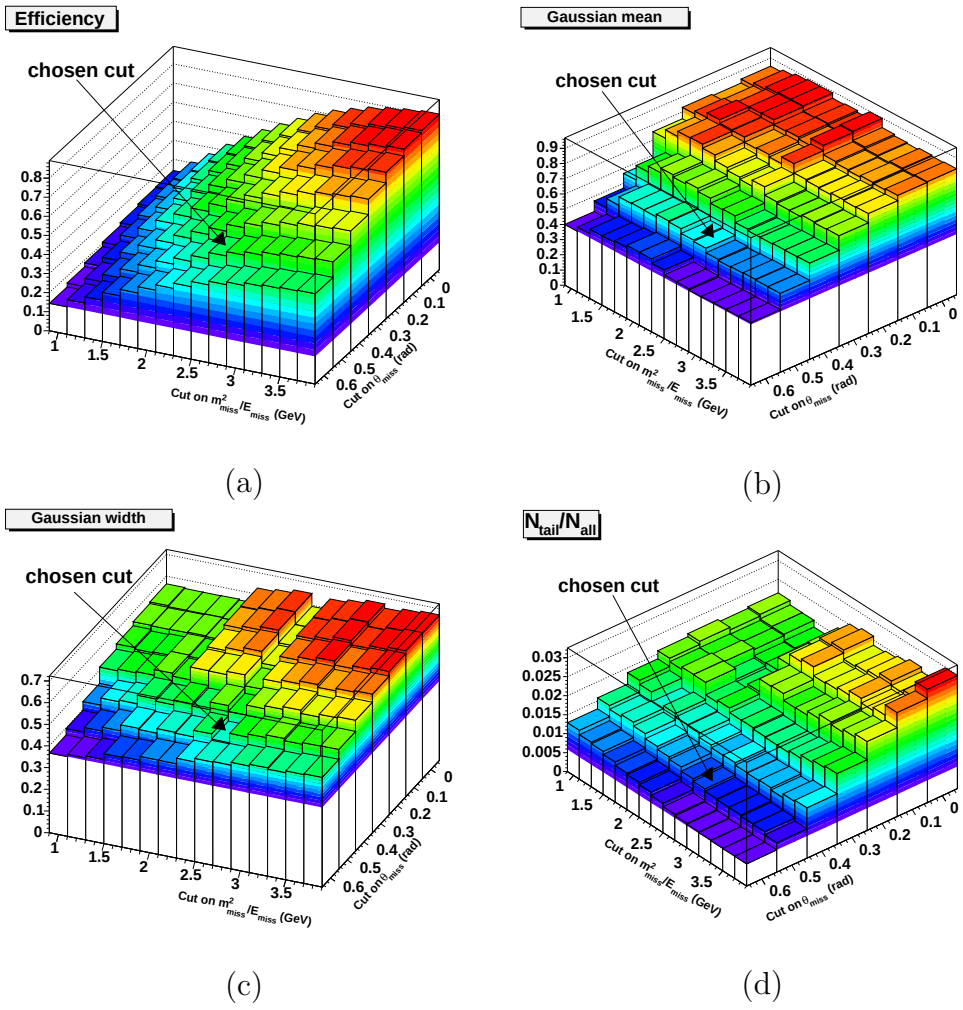

Figure 3: Characteristic quantities of ν momentum resolution for all combinations of cuts on m^2_{miss}/E_{miss} and θ_{miss}. (a) Signal efficiency with preselection, (b) Peak Gaussian mean μ_{peak}, (c) Peak Gaussian width σ_{peak}, and (d) the ratio $\frac{N_{tail}}{N_{all}}$. Similar plots were used with the q^2 resolution to determine the optimal cut.

Sets of Cuts					$\lvert\vec{p}_{miss}\rvert - \lvert\vec{p}_{\nu,true}\rvert$ (GeV)			$q^2_{reco.} - q^2_{true}$ (GeV)		
	Q_{tot}	θ_{miss} (rad)	$\frac{m^2_{miss}}{E_{miss}}$ (GeV)	Signal Efficiency	σ_{peak}	μ_{peak}	$\frac{N_{tail}}{N_{all}}$	σ_{peak}	μ_{peak}	$\frac{N_{tail}}{N_{all}}$
No Cut:	-	-	-	1	0.66	0.848	0.03	1.659	0.474	0.41
Chosen Cuts:	≤ 1	> 0.5	< 2.6	0.552	0.481	0.554	0.010	1.556	0.0192	0.172
Cuts w/ Similar Eff.:	≤ 1	> 0	< 1.8	0.574	0.556	0.889	0.0187	1.834	0.489	0.27
Cuts w/ Similar Eff.:	≤ 1	> 0.3	< 2	0.559	0.597	0.783	0.0178	1.911	0.27	0.241

Table 1: Four combinations of m^2_{miss}/E_{miss}, θ_{miss}, and Q_{tot} cuts with their effect on ν resolutions and signal efficiencies. The chosen set of cuts is compared to the uncut signal Monte Carlo sample along with two other sets of cuts with similar signal efficiencies

with a charm meson in the final state. The continuum background has a more jet-like topology than $B\bar{B}$ events, which are isotropic in the center-of-mass frame. The continuum background is therefore significantly suppressed by preselection. However, preselection is not as effective on $B \to X_c l\nu$ decays, which are also much more abundant than the signal. In addition there is background from other $B \to X_u l\nu$ modes where X_u is $\pi^{\pm}, \pi^0, \rho^{\pm}, \rho^0$, etc. Even after applying the neutrino reconstruction cuts, the background completely overwhelms the signal (Fig. 4). Selection criteria on top of the neutrino reconstruction cuts must be applied to reduce these various backgrounds with respect to the $B \to \omega l\nu$ signal.

We first studied the agreement between Monte Carlo and BaBar data for the two main background sources by comparing them using $B \to X_c l\nu$ and continuum enhanced samples. There was a relatively uniform normalization discrepancy in the continuum background, which may be caused by unsimulated continuum processes in the Monte Carlo. We simply scaled the continuum background by a factor of 1.1 in order to match the data. The shapes of the distributions for several kinematic variables in the $B \to X_c l\nu$ enhanced sample were also slightly different between data and Monte Carlo (at the 10% level). Within the scope of this study, we could not further investigate these deviations.

We define several variables that characterize each reconstructed event and will be used for selection cuts. The first three variables below describe the topology of the event.

- $|\cos\theta_{thrust}|$, where θ_{thrust} is the angle between the thrust axis [5] of the so-called Y system, consisting of the ω and lepton, and the thrust axis of the rest of the event. Here the thrust axis is the direction that maximizes the total longitudinal components of the particle momenta.

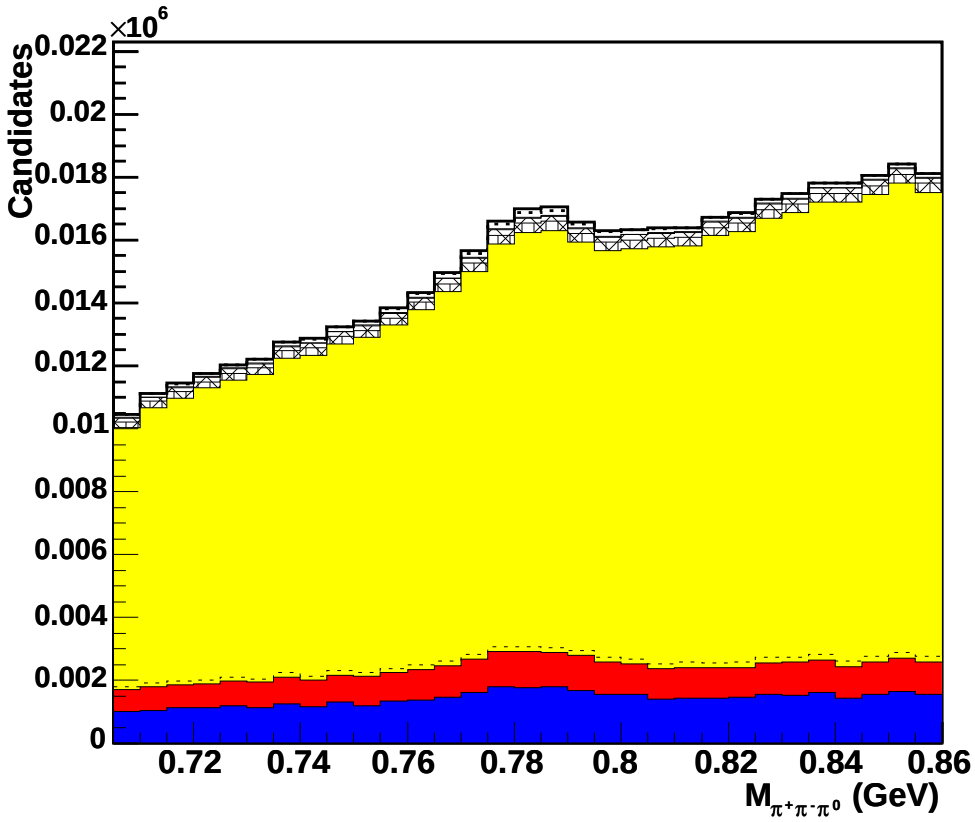

Figure 4: Invariant mass $m_{\pi^+\pi^-\pi^0}$ after only preselection and neutrino reconstruction cuts. Red and blue histograms are $e^+e^- \to q\bar{q}$ events with a real and fake lepton, respectively. Yellow histograms are $B\bar{B}$ background, dominated by $B \to X_c l\nu$ decays (above dotted line). Hatched histograms are other $B \to X_u l\nu$ decays. Simulated signal is shown as white histogram with the contribution from combinatoric signal (see last sentence before Sec. 3.3 for definition) marked as dotted line.

This variable peaks around 1 for jet-like events like $e^+e^- \to q\bar{q}$.

- $L2 = \sum_i |\vec{p}_i^*| \cos^2 \theta_i^*$ where $|\vec{p}_i^*|$ is the momentum of the i^{th} particle in the center-of-mass frame, and θ_i^* is the angle of the momentum with the thrust axis of the Y system. This quantity is large for jet-like events and small for isotropic ones such as semileptonic B decays.

- $R2$: the ratio of the 2^{nd} to 0^{th} Fox-Wolfram moments [6]. It is close to 0 for isotropic events and close to 1 for jet-like events.

- The cosine of the angle between the Y system and the B meson, given by

$$\cos\theta_{BY} = (2E_B^* E_Y^* - M_B^2 - M_Y^2)/(2|\vec{p}_B^*||\vec{p}_Y^*|), \tag{5}$$

  where the B momentum and energy are calculated from the known beam four-momenta and the Y momentum and energy are determined through the reconstruction of the lepton and ω. For correctly constructed $B \to \omega l\nu$ decays, $\cos\theta_{BY}$ should be between -1 and 1 so that θ_{BY} corresponds to a physical angle. The backgrounds, on the other hand, should have a broader distribution.

- $\Delta E = E_B^* - \sqrt{s}/2$, where E_B^* is the energy of the reconstructed B meson and $\sqrt{s}$ is the mass of the $\Upsilon(4S)$.

- $m_{ES} = \sqrt{s/4 - (\vec{p}_B^*)^2}$, the beam energy substituted mass of the reconstructed B meson.

We use the preselected Monte Carlo samples to determine which variables show a discrimination between signal and background and are therefore useful for selection cuts. We first optimized cuts on topology and kinematics variables. The topology variables showed significant differences between the signal and continuum backgrounds, while kinematic variables such as lepton

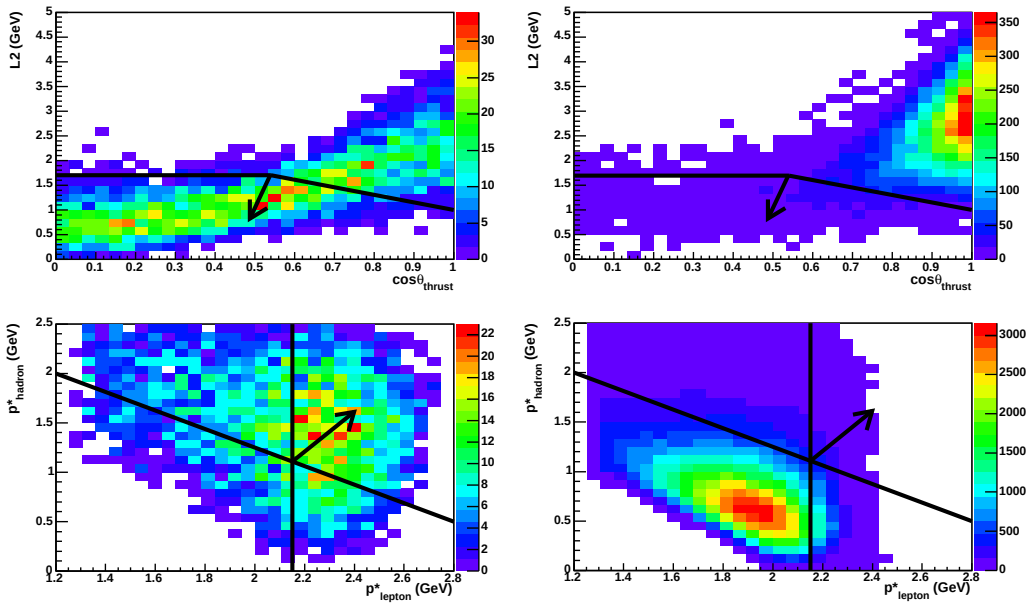

Figure 5: Top: Distributions of L2 vs. $\cos\theta_{thrust}$ for simulated signal (left) and continuum background (right). Bottom: Distributions of lepton vs. hadron momentum for simulated signal (left) and $B \to X_c l\nu$ background (right). Black arrow points to region selected.

and hadron momentum were very effective in suppressing other semileptonic decays (see Fig. 5). For example, $B \to X_c l\nu$ background tends to have lower lepton and hadron momenta than the $B \to \omega l\nu$ signal due to the heavier quark produced. Distributions for some of these variables can be found in Fig. 6. A list of selection cuts along with signal efficiencies and approximate amount of background reduction is given in Table 2. Fig. 6 also compares simulation with data selected from a sample of 83 million $B\bar{B}$ events. Simulated samples have been scaled to the data statistics. We see reasonable agreement between data and simulation and a clear excess of signal events above the dominant background. There are also contributions from other $B \to X_u l\nu$ decays, as well as a contribution from signal decays where the reconstructed ω includes a background pion or photon ("combinatoric sig-

nal").

3.3 Signal Extraction

After all other cuts have been optimized, we extract the $B \to \omega l\nu$ signal from the $\Delta E, m_{ES}$, and $m_{\pi^+\pi^-\pi^0}$ distributions. For signal decays, we expect ΔE to be close to 0; m_{ES} and $m_{\pi^+\pi^-\pi^0}$ should correspond to the B mass and the ω mass, respectively. We require that $-0.3 < \Delta E < 0.5$ GeV, $m_{ES} > 5.23$ GeV, and $0.75 < m_{\pi^+\pi^-\pi^0} < 0.81$ GeV. These three cuts had the most significant effects on our signal-to-background ratio. Fig. 6 and 7 show the distributions of these variables with their corresponding cuts.

4 Results and Discussion

After all cuts we were able to see a distinct mass peak around the omega mass of 782 MeV in the $m_{\pi^+\pi^-\pi^0}$ distribution (Fig. 7). This shows that we have effectively reduced the background and can extract the desired $B \to \omega l\nu$ signal. The final Monte Carlo signal efficiency is of the order of 1%, while the various backgrounds have been reduced by roughly 10^{-4} to 10^{-6}. A comparison between the effects of signal extraction on the Monte Carlo signal and background is given in Table 3. The final number of signal events predicted by the Monte Carlo simulation is 133, and the total number of expected background events is 195, giving a signal-to-background ratio of 0.68. This ratio is more than sufficient for isolating the signal processes above background uncertainties.

We determine the number of signal events in the data by subtracting out the Monte Carlo simulated background distributions. We find 115 ± 19 $B \to \omega l\nu$ decays in the data, where the error includes the statistical

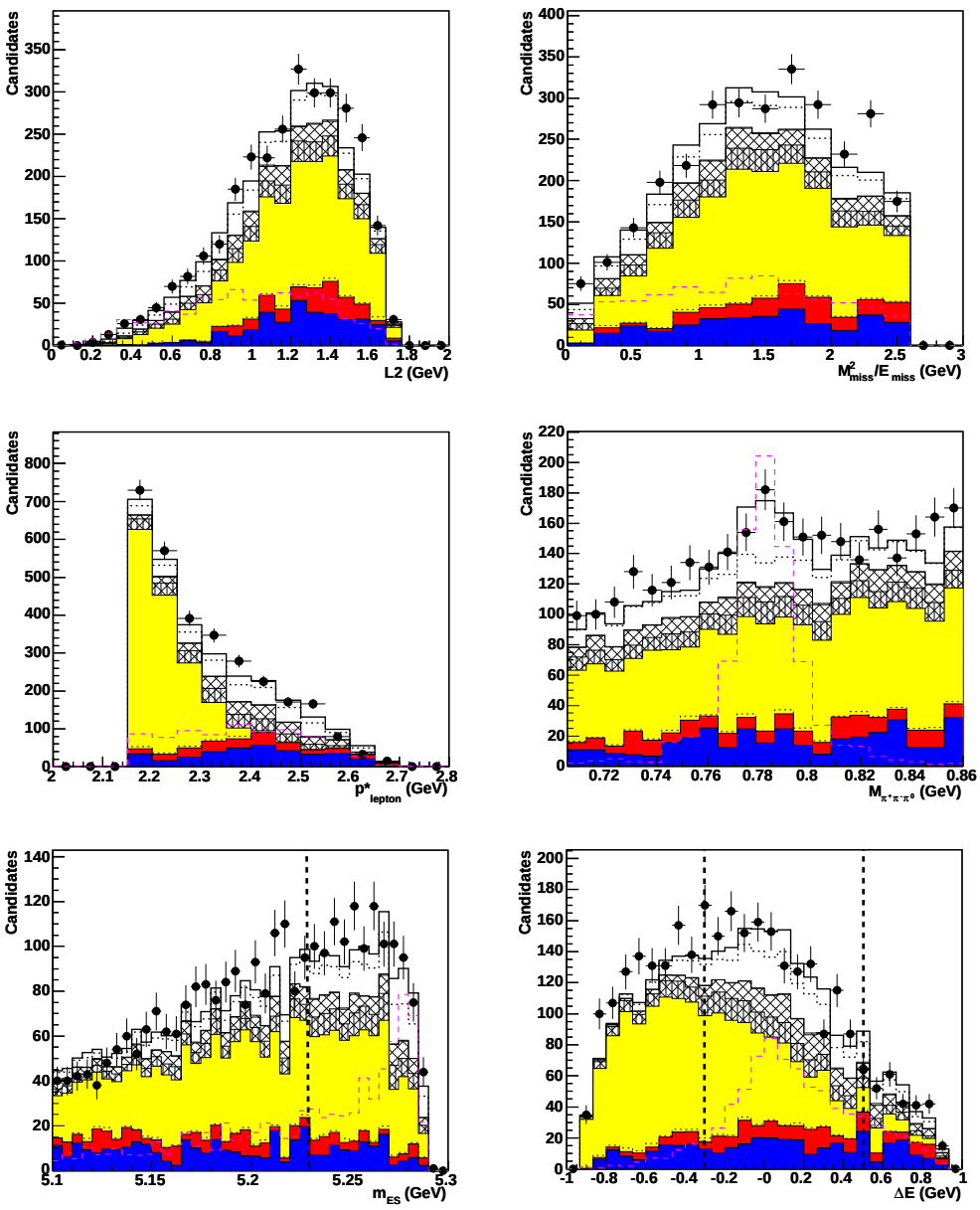

Figure 6: Distributions before signal extraction for six variables used in the selection cuts. ΔE and m_{ES} are shown with corresponding cuts indicated by vertical lines. Monte Carlo simulation (histograms) is compared to BaBar data (points). Magenta dashed histograms with arbitrary normalization indicate the signal shapes. See Fig. 4 caption for details.

	signal	$B \to X_c l\nu$	$B \to X_u l\nu$	$e^+e^- \to q\bar{q}$
	Efficiencies of preselection(%)			
preselection	35	1.8	6.1	0.4
	Efficiencies of individual cuts on top of preselection(%)			
$\|p_\nu\| > 0.7$ GeV	96	99	99	85
neutrino reconstruction	50	29	42	33
$R2 < 0.4$	92	99	97	64
$\|\cos\theta_{BY}\| < 1$	92	66	71	73
$p^*_{hadron} + 0.94p^*_{lepton} > 3.125$ GeV; $p^*_{lepton} > 2.15$ GeV	43	1.4	11	31
$L2 + 1.5\cos\theta_{thrust} < 2.5; L2 < 1.7$ GeV	63	47	49	7.8

Table 2: Cut efficiencies for simulated signal and background samples.

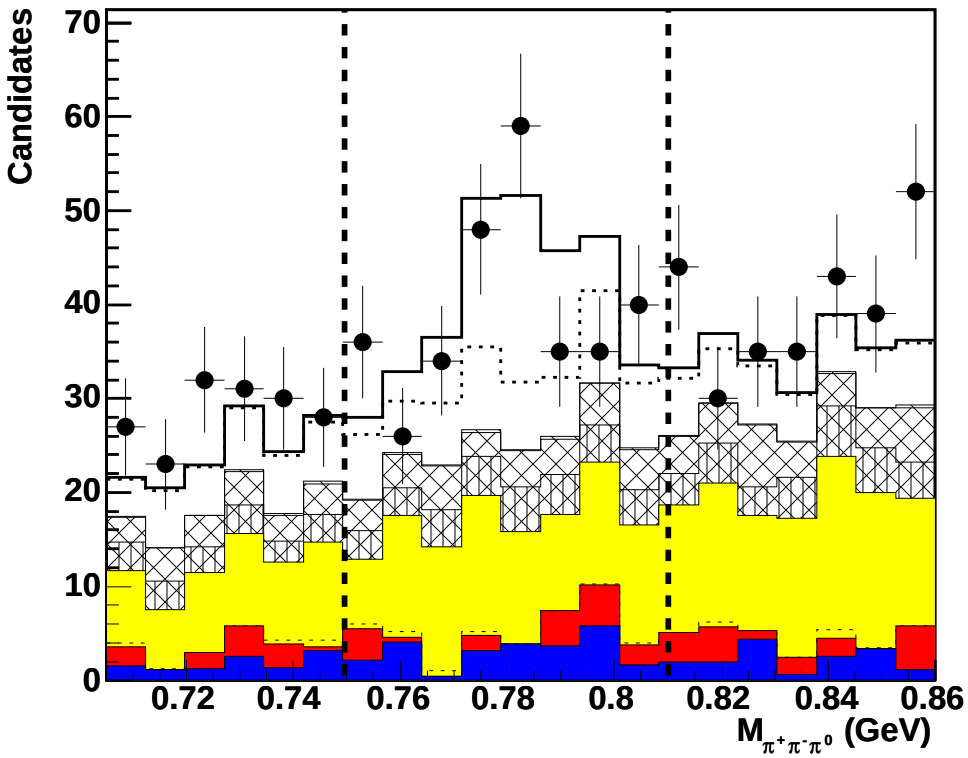

Figure 7: Invariant mass $m_{\pi^+\pi^-\pi^0}$ after all selection cuts but the one on the mass itself. The final mass cut is indicated as vertical lines. The raggedness of the continuum background distribution is due to the low statistics of the Monte Carlo sample. See Fig. 4 caption for details.

	Before Sig. Extr.	After Sig. Extr.
Signal Events	482	133
Background Events	2386	195
Signal-to-background ratio	0.20	0.68
Signal Efficiency (approximate)	0.04	0.01
Background Efficiency (approximate)	10^{-5}	10^{-6}

Table 3: Effects of signal extraction along with final numbers of events and efficiencies.

uncertainties of the data and Monte Carlo samples.

We hope to use the work presented here to calculate the $B \to \omega l \nu$ branching fraction, which can be obtained using the exact signal efficiency along with the number of signal events in the data. Another feature that calls for further investigation is the discrepancies between the data and $B \to X_c l \nu$ and continuum backgrounds observed in the dedicated background-enhanced samples. Eventually, the analysis of this decay mode can be used to extract the CKM matrix element $|V_{ub}|$ and thus constrain the Unitarity Triangle.

5 Acknowledgements

We would like to thank the Department of Energy, Office of Science and SLAC for this opportunity to participate in the SULI program. We would especially like to express our gratitude to our mentor, Jochen Dingfelder, who always took time out of his extremely busy schedule to help us with our programming and explain the physics behind what we were doing. We would also like to thank Vera Lüth, Mike Kelsey, Kai Yi, and the rest of our colleagues in Group C for providing valuable help and advice.

References

[1] L. Wolfenstein, *Phys. Rev. Lett.* **51**, 1945 (1983).

[2] *BABAR* Collaboration, B. Aubert *et al.*, hep-ex/0507003, (Submitted to Phys. Rev. Lett. D Rapid Communications).

[3] Belle Collaboration, C. Schwanda *et al.*, Phys. Rev. Lett. **93**, 131803 (2004).

[4] A.J. Weinstein, "Study of Exclusive Charmless Semileptonic Decays of the B Meson", PhD thesis, Stanford Linear Accelerator Center (2004).

[5] E. Farhi, *Phys. Rev. Lett.* **39**, 1587(1977).

[6] G.C. Fox and S. Wolfram, *Nucl. Phys.* **B149**, 413 (1979).